Organic & Biomolecular Chemistry

Accepted Manuscript

This article can be cited before page numbers have been issued, to do this please use: M. Grote, S. Kushnir, N. Pryk, D. Möller, J. Erver, A. Ismail-Ali and F. Schulz, *Org. Biomol. Chem.*, 2019, DOI: 10.1039/C9OB00831D.

ROYAL SOCIETY OF CHEMISTRY

rsc.li/obc

View Article Online
DOI: 10.1039/C9OB00831D

Identification of Crucial Bottlenecks in Engineered Polyketide Biosynthesis

*Marius Grote, Susanna Kushnir, Niclas Pryk, David Möller, Julian Erver, Ahmed Ismail-Ali, Frank Schulz**

Affiliation

Organische Chemie 1
AG Naturstoffchemie und -biochemie
Fakultät für Chemie und Biochemie
Ruhr-Universität Bochum
Universitätsstraße 150
44780 Bochum, Germany

ABSTRACT

The concept of combinatorial biosynthesis promises access to compound libraries based on privileged natural scaffolds. Ever since the elucidation of the biosynthetic pathway towards the antibiotic erythromycin A in 1990, the predictable manipulation of type I polyketide synthase megaenzymes was investigated. However, this goal was rarely reached beyond simplified model systems. In this study, we identify the intermediates in the biosynthesis of the polyether monensin and numerous mutated variants using a targeted metabolomics approach. We investigate the biosynthetic flow of intermediates and use the experimental setup to reveal the presence of selectivity filters in polyketide synthases. These obstruct the processing of non-native intermediates in the enzymatic assembly line. Thereby we question the concept of a truly modular organization of polyketide synthases and highlight obstacles in substrate channeling along the cascade. In the search for the molecular origin of a selectivity filter, we investigate the role of different thioesterases in the monensin gene cluster and the connection between ketosynthase sequence motifs and incoming substrate structures. Furthermore, we demonstrate that the selectivity filters do not apply to new-to-nature side-chains in nascent polyketides, showing that the acceptance of these is not generally limited by downstream modules.

INTRODUCTION

Biosynthesis of polyketides on type I polyketide synthases (PKS) follows the colinearity rule, in which the structure of the biosynthetic product is determined by the type and location of respective catalytic domains.[1] The monensin PKS is a member of this enzyme family and comprises a loading module and twelve extender modules on eight proteins with 2,239 to 4,133 amino acids and a total molecular weight of about 4 MDa.[2, 3] In a PKS, each module catalyzes typically one elongation step on the nascent polyketide chain as well as an individually different number of reductive steps (Fig. 1B). The minimal

View Article Online
DOI: 10.1039/C9OB00831D

set of catalytic domains in a canonical module towards a reduced polyketide such as monensin is composed of a ketosynthase (KS), an acyltransferase (AT) and an acyl carrier protein (ACP). The oxidation state is determined by the optional presence of a ketoreductase (KR), a dehydratase (DH) and an enoylreductase (ER) domain which reduce the primary β-ketothioester product in a stepwise fashion, analogous to fatty acid biosynthesis.[4]

This apparent modular organization of PKS has been utilized for the engineered biosynthesis of polyketide derivatives. Combinatorial biosynthesis potentially enables the generation of highly diverse and otherwise hardly accessible new-to-nature compounds, yet it often suffers from low fermentation yields and poor predictability of the experimental outcome.[5, 6]

The monensin PKS orchestrates 71 catalytic steps on the way from a malonyl-coenzyme A starter unit towards the fully assembled backbone of the natural product, the shunt product premonensin described previously.[7] However, this biosynthetic pathway is remarkably specific and after extensive post-PKS processing, delivers monensin A and B as the dominant products. At the same time, the monensin PKS reveals a significant catalytic promiscuity, most prominently in the AT domain in module 5 (monAT5), which was shown to accept a range of different extender units if these are supplied to the fermentation medium.[8-10] On the other hand, the targeted inactivation of reducing domains in the monensin PKS often resulted in a drop of fermentation yields towards the modified products.[11]

The moderate to high fidelity on PKS assembly lines is ascribed to either the substrate specificity of individual catalytic domains or a precise domain-domain interaction pattern which ensures the channeling of the nascent polyketide chain in the correct order of catalytic events.[5, 12-14] The exclusive use of targeted point mutations in the engineering of the monensin PKS, however, minimizes the structural disturbance of the large PKS multienzyme complexes,[15] therefore, diminished fermentation yields in such experiments could potentially be attributed to an intrinsic substrate specificity of individual PKS segments.

We launched a comparative investigation of differently mutated variants of *Streptomyces cinnamonensis* to investigate potential obstacles in the channeling of the nascent polyketide chain in an engineered biosynthesis. Alterations targeted both the redox pattern and the extender unit flexibility of the monensin PKS, using the shunt product premonensin as a model system.

Consequently, two different experimental approaches seemed applicable: Synthetic chain terminators to capture intermediates[16-18] or the direct detection of spontaneously or enzymatically released intermediates as hop-off products.[19, 20]

RESULTS

Firstly, monensin biosynthesis in the wild-type strain *S. cinnamonensis* ATCC 15413 was analyzed for spontaneous hop-off products from the assembly line via LC-HRMS. The biosynthetic pathway, including a complex post-PKS processing towards monensin, is described to proceed via fully ACP-attached intermediates. Product release is assumed to run via a non-canonical thioesterase[2, 3, 21] and no nascent polyketide intermediates towards monensin were detectable. However, when the mutated strain *S. cinnamonsis* A495 (*S. cinnamonsis* ATCC 15413 ΔmonCIΔmonBI/II[7]) was fermented in an analogous manner, the release of the previously described new-to-nature product premonensin by

View Article Online
DOI: 10.1039/C9OB00831D

this variant was not as efficient as for monensin in the case of the wild type. Instead, the intermediate product for each module from module 4 upwards was detectable in the fermentation extract (Fig. 1).

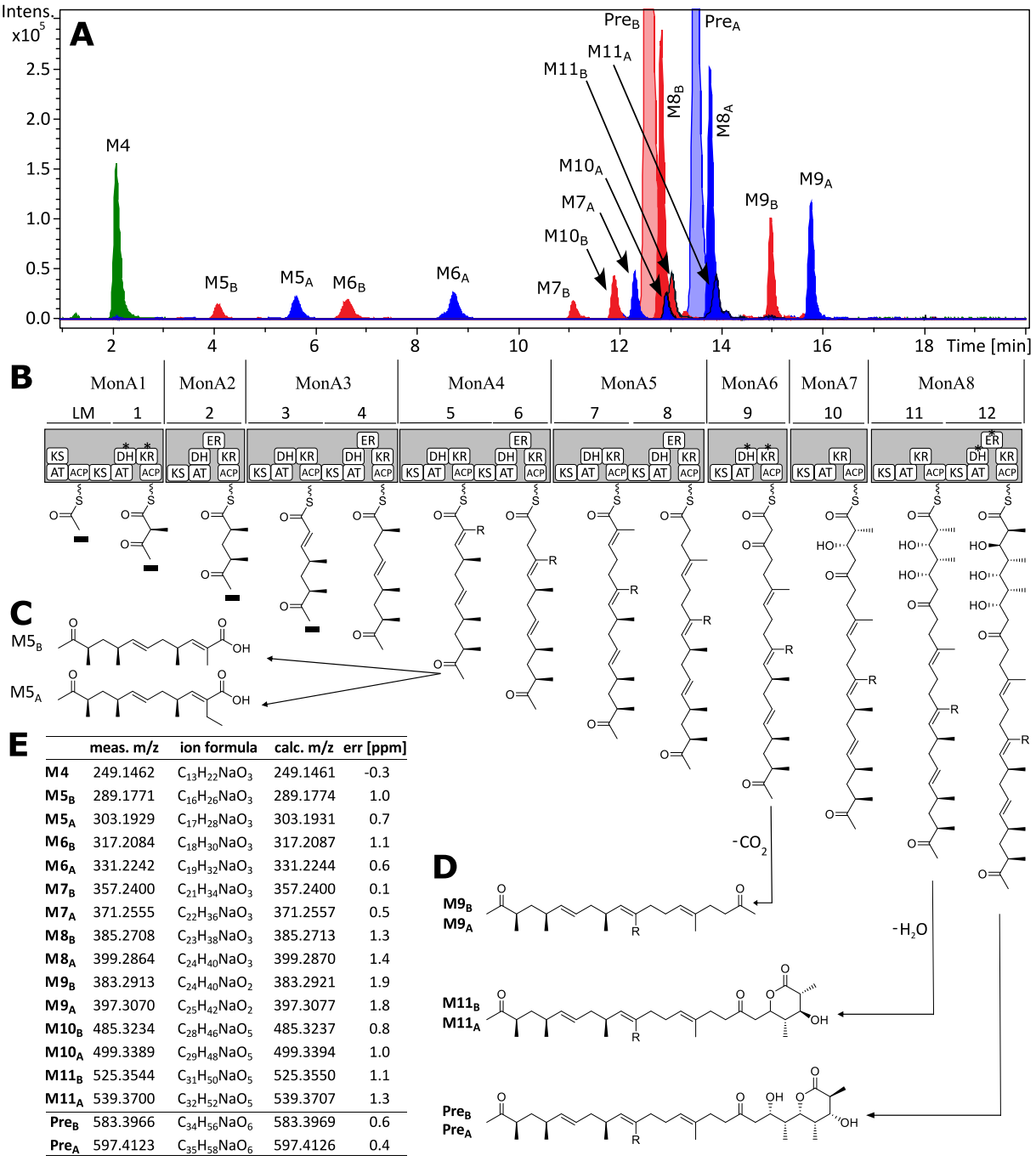

E

	meas. m/z	ion formula	calc. m/z	err [ppm]
M4	249.1462	$C_{13}H_{22}NaO_3$	249.1461	-0.3
M5$_B$	289.1771	$C_{16}H_{26}NaO_3$	289.1774	1.0
M5$_A$	303.1929	$C_{17}H_{28}NaO_3$	303.1931	0.7
M6$_B$	317.2084	$C_{18}H_{30}NaO_3$	317.2087	1.1
M6$_A$	331.2242	$C_{19}H_{32}NaO_3$	331.2244	0.6
M7$_B$	357.2400	$C_{21}H_{34}NaO_3$	357.2400	0.1
M7$_A$	371.2555	$C_{22}H_{36}NaO_3$	371.2557	0.5
M8$_B$	385.2708	$C_{23}H_{38}NaO_3$	385.2713	1.3
M8$_A$	399.2864	$C_{24}H_{40}NaO_3$	399.2870	1.4
M9$_B$	383.2913	$C_{24}H_{40}NaO_2$	383.2921	1.9
M9$_A$	397.3070	$C_{25}H_{42}NaO_2$	397.3077	1.8
M10$_B$	485.3234	$C_{28}H_{46}NaO_5$	485.3237	0.8
M10$_A$	499.3389	$C_{29}H_{48}NaO_5$	499.3394	1.0
M11$_B$	525.3544	$C_{31}H_{50}NaO_5$	525.3550	1.1
M11$_A$	539.3700	$C_{32}H_{52}NaO_5$	539.3707	1.3
Pre$_B$	583.3966	$C_{34}H_{56}NaO_6$	583.3969	0.6
Pre$_A$	597.4123	$C_{35}H_{58}NaO_6$	597.4126	0.4

Figure 1: A. Extracted ion chromatograms ([M+Na]$^+$ ± 0.005 m/z) indicating the hop-off products released from the assembly line as free acids. The hop-off products from different modules (M) were detected via LC-HRMS in extracts from fermentations of *S. cinnamonensis* A495. Reductive domains labeled with an asterisk are evolutionarily inactivated in the native assembly line. The fermentation products were absorbed *in situ* onto XAD16 resin in the fermentation broth, which was subsequently eluted using ethyl acetate. In module 5, a promiscuous acyl transferase incorporates two different extender units into the nascent polyketide chain, leading to premonensin A and B (Pre$_A$/Pre$_B$). Likewise, intermediates from module 5 upwards arise as A (red)- and B (blue)-derivatives (premonensin B: R = methyl; premonensin A: R = ethyl), exemplarily shown for the M5 intermediate (**C**). **B.** Modular assembly line of the monensin gene cluster consisting of a loading module (LM) and 12 elongation modules encoded on 8 separate proteins (MonA1-MonA8). Instead of passing on, spontaneous hydrolysis of the nascent polyketide results in hop-off products M4 to M11. Hop-off products M6$_{A/B}$ were previously isolated and fully characterized by NMR spectroscopy.[9] Early intermediates labelled with "–" do not

View Article Online
DOI: 10.1039/C9OB00831D

bind reliably to XAD16 resins and, thus, are not included in the analysis. KS: Ketosynthase. DH: Dehydratase. ER: Enoylreduktase. KR: Ketoreductase. AT: Acyl transferase. ACP: Acyl carrier protein. **D.** The β-ketone hop-off product M9 was only detected in its decarboxylated form ($M9_{A/B}$). Intermediates released from module 11 were detected in the form of the corresponding lactones, similar to that in the release of the final products Pre_A and Pre_B. Linear intermediates were detected in variable, but low, abundancies for both. **E.** HRMS data from the main adduct $[M+Na]^+$ of each intermediate. Accurate masses for further adducts, mSigma values[22-24] and MS/MS-fragmentation patterns are described in the SI (chapter 5).

The inactivation of post-PKS enzymes in monensin biosynthesis not only leads to the anticipated product alteration but also appears to introduce a strong congestion in the pathway, leading to a release of intermediates through the spontaneous competing hydrolysis *en route* to downstream modules. This supports the model of the dedicated thioesterase (TE) monCII for product release in monensin biosynthesis[21] and suggests that the shunt product premonensin is formed by spontaneous lactonization and, hence, cleavage from the ACP in the final module.

The data presented here unequivocally confirm the biosynthetic pathway for premonensin and support the current model for ACP-aided post-PKS processing (*vide supra*). This is in accord with the comparably low yields in premonensin fermentation as the release of this shunt product from a trans-acting ACP proceeds spontaneously and is not TE-mediated. The most abundant intermediates arise from hydrolysis after modules 4, 8 and 9 (Fig. 1A), henceforth named M4, M8 and M9. All shunt products described here are absent in the wild-type strain, indicating that the release of the final product is rate-limiting in the modified biosynthetic pathway towards premonensin.

Intermediates in Redox Derivative Biosynthesis

We next turned our attention to the biosynthesis of the recently reported premonensin redox-derivative $ER2^0$.[11] It is biosynthesized via a mutated monensin PKS, carrying two adjacent point mutations in the second extension module through which its ER domain loses most of its activity. As the main products of the fermentation are the redox derivatives, the loss-of-activity mutation causes the reduction of the intermediate C=C bond to be significantly slower than the transfer of the nascent polyketide derivative to the downstream module 3. The typical fermentation yield of premonensin $ER2^0$ is at about 10 % of the value obtained for the unmodified version, rendering it the most productive variant generated in a library of premonensin redox-derivatives.[11]

When the fermentation products of *S. cinnamonensis* A495-$ER2^0$ were analyzed using the same methodology, an analogous yet significantly different pattern was found in the abundance of intermediates (Fig. 2).

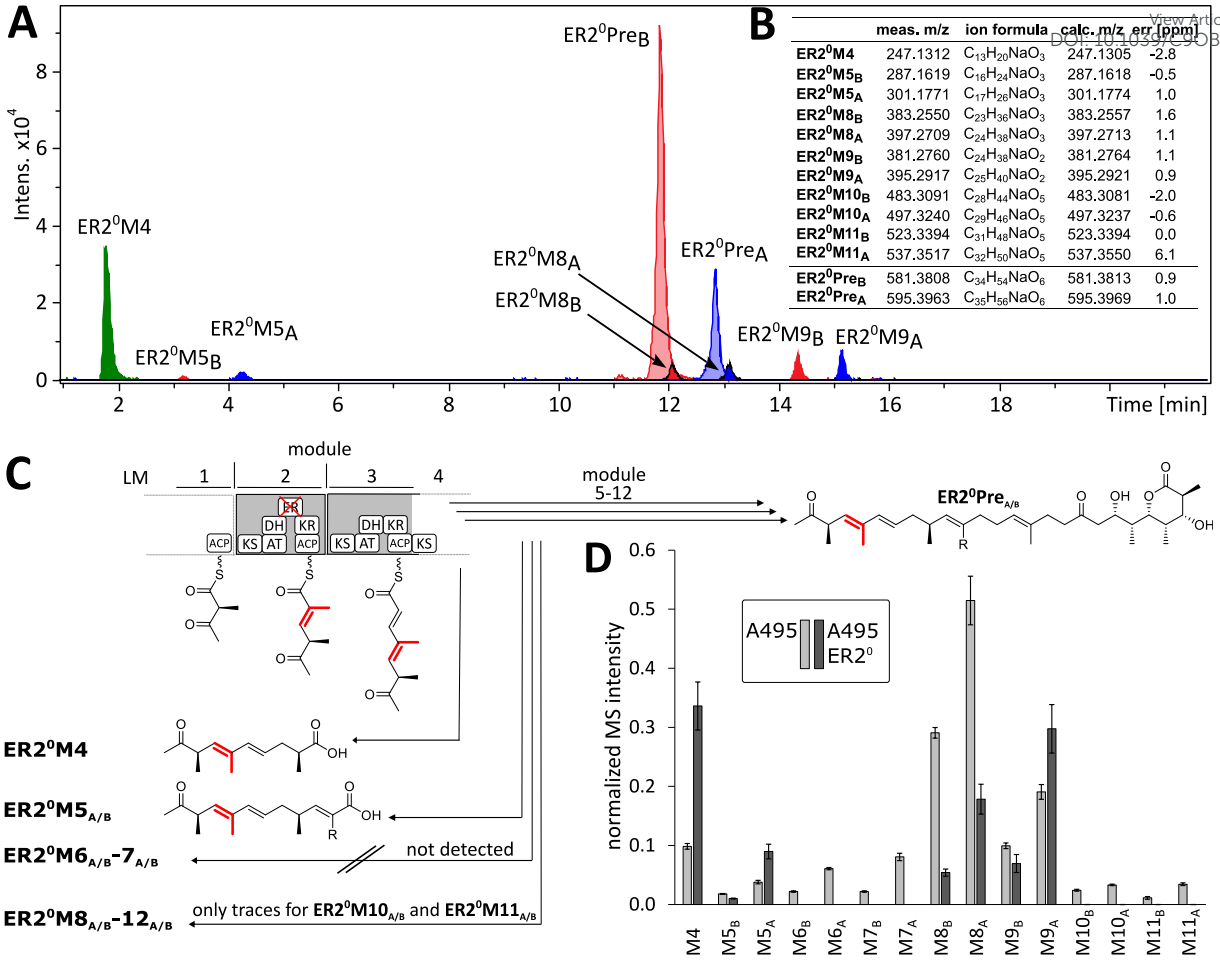

Figure 2: A. Extracted ion chromatograms ([M+Na]$^+$ ± 0.005 m/z) indicating the hop-off products released from different modules (M) in a fermentation of *S. cinnamonensis* A495-ER2^0. The redox derivatives of premonensin are labelled as ER2^{0}Pre$_{A/B}$ (A: R = ethyl, B: R = methyl). While the relative abundance of ER2^{0}M4 in comparison to the final product rises, hop-off products from modules 6 and 7 could not be detected, and only trace amounts were found for M10 and M11. **B.** HRMS-data of the hop-off products (ER2^{0}M) detected and the final redox derivatives ER2^{0}Pre$_{A/B}$. Further characterization is found in the SI, chapter 5. **C.** Clipping from the assembly line indicating the ER-inactivating point mutation in module 2. This results in the incomplete reduction of the polyketide before it is passed on to the downstream module. **D.** Comparison of the MS signal intensity of individual intermediates in *S. cinnamonensis* A495 and A495-ER2^0, normalized to the signal intensity of the respective biosynthetic end products. Error bars represent the mean standard deviation over four independent clones.

The abundance of the early intermediate ER2^{0}M4 was significantly increased over the later products. Intermediates ER2^{0}M6 and ER2^{0}M7 were released below the detection limit, in contrast to the fermentation of unmodified premonensin, while the relative abundance of ER2^{0}M5$_{A/B}$ was slightly higher than its reduced counterpart in the control fermentation of unmodified premonensin. Intermediates beginning from module 8 could again be detected, albeit only in traces of ER2^{0}M10$_{A/B}$ and ER2^{0}M11$_{A/B}$. This suggests a significant rate-limitation in early modules, leading to a lowered occupation of ACP in downstream modules.

View Article Online
DOI: 10.1039/C9OB00831D

Ketoreductase Null Mutants

This prompted us to investigate the biosynthesis of those premonensin derivatives in variants of *S. cinnamonensis* A495 that we previously identified as non- or low-productive.[11] We began with KR variants from modules 4 to 6, of which $KR4^0$ and $KR6^0$ yielded the corresponding premonensin derivatives (premonensin $KR4^0_{A/B}$ and $KR6^0_{A/B}$) in non-isolatable amounts, whereas variant $KR5^0$ did not yield any detectable quantity of premonensin $KR5^0_{A/B}$. The intermediates in the respective mutated module were identified in all three examples ($KR4^0M4$, $KR5^0M5_{A/B}$ and $KR6^0M6_{A/B}$). No hop-off products from downstream modules were detected identifying the transfer of the derivatized intermediate to the respective downstream module or its elongation in that module as rate-limiting steps (Fig. 3).

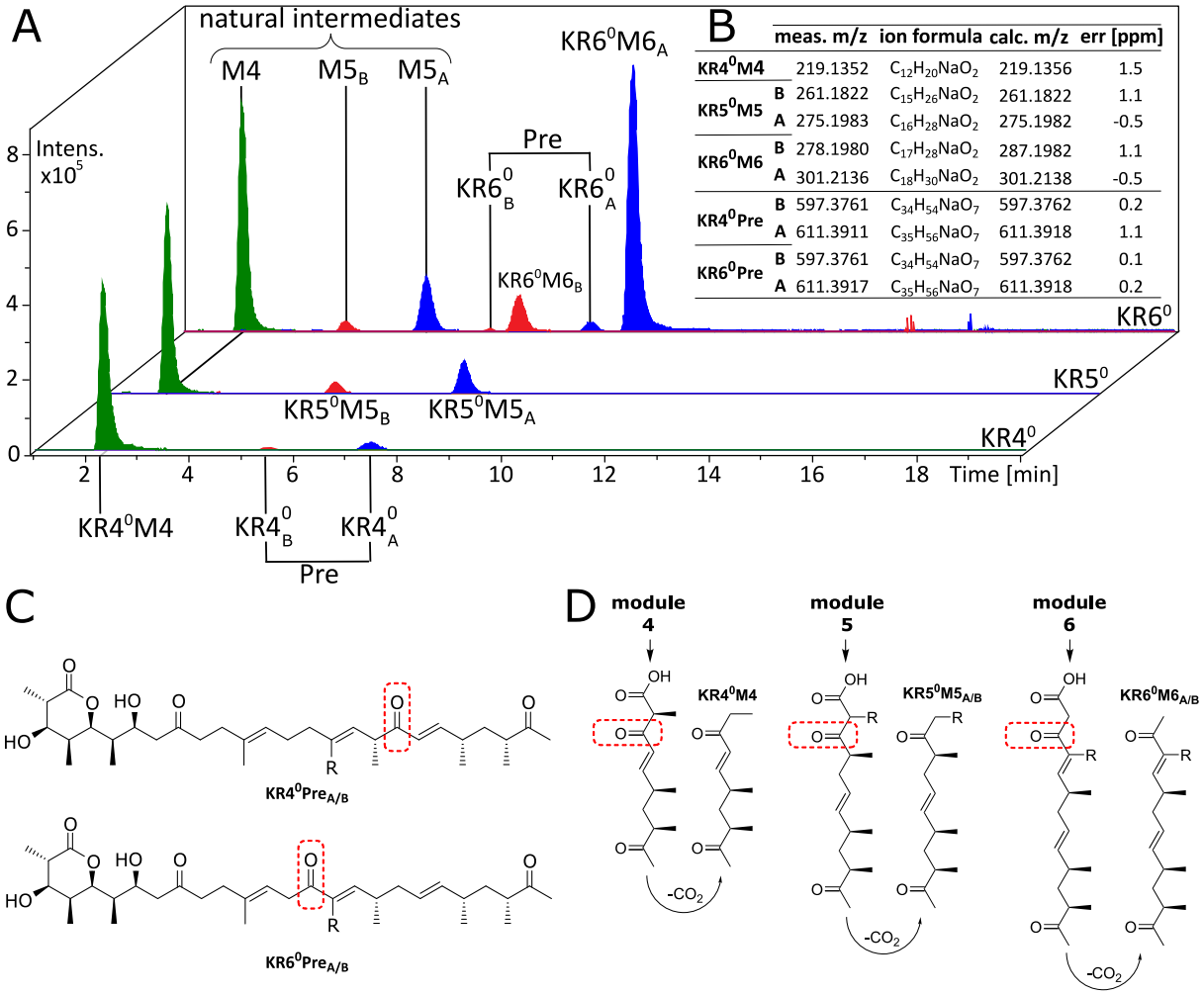

Figure 3: A. Extracted ion chromatograms ($[M+Na]^+ \pm 0.005$ m/z) showing the hop-off products in fermentations of different KR^0 variants of *S. cinnamonensis* A495. As expected, the β-ketoacids were completely detected as decarboxylated compounds. The native intermediates were detectable until ahead of the mutated module. $KR4^0$Pre: premonensin $KR4^0_{A/B}$. $KR6^0$Pre: premonensin $KR6^0_{A/B}$ **B.** HRMS data of the decarboxylated hop-off products ($KR4^0M4$, $KR5^0M5_{A/B}$, $KR6^0M6_{A/B}$) and the final shunt products premonensin $KR4^0_{A/B}$ and premonensin $KR6^0_{A/B}$. Further HRMS-characterization of all compounds can be found in the SI chapter 5. **C.** Structures of the redox derivatives $KR4^0$Pre and $KR6^0$Pre. **D.** Structures of the decarboxylated intermediates released from the assembly line in the three KR^0 mutants.

View Article Online
DOI: 10.1039/C9OB00831D

Intermediate KR6^{0}M6$_{A/B}$ accumulated strongly in *S. cinnamonensis* A495 KR6^0, in contrast to fermentations of both *S. cinnamonensis* A495 and the ER2^0 variant, emphasizing the rate-limitation induced by the redox-derivatization. Hydrolysis of the respective intermediate largely outcompetes its transfer to module 7. This appears to limit the productivity of the overall assembly line towards the new-to-nature fermentation product in each of the KR^0 variants investigated.

This led us to the introduction of analogous KR^0 mutations in the final modules 11 and 12, which had not been reported previously. The KR11^{0}M11$_{A/B}$ intermediates in variant KR11^0 show some accumulation ahead of their transfer to module 12 in compliance with the observations of targeted earlier modules; the biosynthesis afterwards proceeds to the predictable final products (SI chapters 4 and 5).

No specific selectivity filter can be deduced for the mutation in module 12 as the final elongation module and, according to the expectations, the engineered biosynthesis delivers the products anticipated in an intensity which is comparable to the premonensin fermentation in the control strain (SI chapters 4 and 5). This indicates that the introduced point-mutation in KR^0 domains does not necessarily compromise the assembly line's structure, but instead, a substrate specific filter appears to exist.

Dehydratase Null Mutants

We next analyzed the cause of the fermentation in DH^0 variants of the premonensin assembly line. DH^0 variants yielded the predicted new-to-nature fermentation products in the majority of cases tested in a previous report,[11] in sharp contrast to KR^0 variants. The productivity, however, was usually too low to allow for the seamless isolation of the premonensin derivatives from the fermentation broths.

Fermentations of *S. cinnamonensis* A495 DH2^0, DH4^0, DH5^0, DH7^0 and DH8^0 were analyzed as described above. In these cases, the limitation induced by the redox-derivatization is not as severe as for KR^0 mutants. In each case, the corresponding premonensin derivative can be detected, however, at significantly diminished intensities. In the case of targeting the DH domain in module 5, both DH5^{0}M5$_{A/B}$ intermediates accumulate strongly similar to analogous KR^0 variants. After the completion of the PKS assembly line, DH5^{0}Pre$_B$ can be detected in a very low intensity, while DH5^{0}Pre$_A$ falls below the detection limit (for chromatograms and HRMS analysis see SI chapters 4 and 5). This indicates a difference in the processing of the two DH5^{0}M5 intermediates in downstream modules. Each DH^0 variant was also found to be "leaky" and produced varying amounts of premonensin A and B as a by-products. This demonstrates that the mutation used for DH domains cannot fully inactivate these, which is in accordance with previous findings.[25]

Enoylreductase Null Mutants

We then turned our attention to ER^0 variants in modules 6 and 8. Both *S. cinnamonensis* A495 ER6^0 and ER8^0 deliver the corresponding premonensin derivatives.[11] The respective intermediates are found throughout the assembly line, with the exception of ER6^{0}M10$_{A/B}$ (for chromatograms and HRMS analysis see SI chapters 4 and 5). The results indicate little limitation from an in-built selectivity filter on ER^0 variant productivity, which is in accordance with our previous observation of a high productivity in these variants.

View Article Online
DOI: 10.1039/C9OB00831D

The General Effect of Null Mutations on Polyketide Synthase Redox Domains

The combined results from mutations in KR, DH and ER domains indicate that a redox-derivatization introduces new rate-limitations in the engineered biosynthesis of premonensin derivatives, which correlates with the low yields in the isolation of the corresponding derivative from fermentation broths (an overview of all detected hop-off intermediates is found in Figure S2). ER^0 redox variants are structurally closest to the wild-type product and are typically tolerated throughout the whole assembly line, albeit they converted with a reduced catalytic processivity. This tendency is still visible for DH^0 variants, however, significant rate-limitations can be identified in several cases. The exact localization of the limiting effect cannot be deduced by the detection of intermediates. However, the productivity loss of the full assembly line is most pronounced in KR^0 variants, which show a strong accumulation of intermediates in the targeted module.

The Effect of Combined Null Mutations on the Assembly Line

We next investigated the combination of redox variations in engineered premonensin biosynthesis. Mutation $ER2^0$ was individually combined with mutations $KR4^0$, $DH5^0$, $KR8^0$ and $DH8^0$. This miniature library combined the productive $ER2^0$ mutation with one productive and one unproductive DH^0 and KR^0 variant, respectively. The assembly line regarding variants $ER2^0KR8^0$ and $ER2^0DH5^0$ ended in the targeted modules 8 and 5, respectively (for chromatograms and HRMS see SI chapter 4 and 5). By contrast, variants $ER2^0KR4^0$ and $ER2^0DH8^0$ gave rise to the corresponding doubly-modified premonensin derivatives (Fig. 4A, E, F), of which premonensin $ER2^0DH8^0$ was chosen for structural characterization. Analysis of the fermentation extract revealed an intrinsic instability of the products by dehydratization, driven by the strong conjugation of the resulting C=C bonds in the respective products (see Fig. 4).

View Article Online
DOI: 10.1039/C9OB00831D

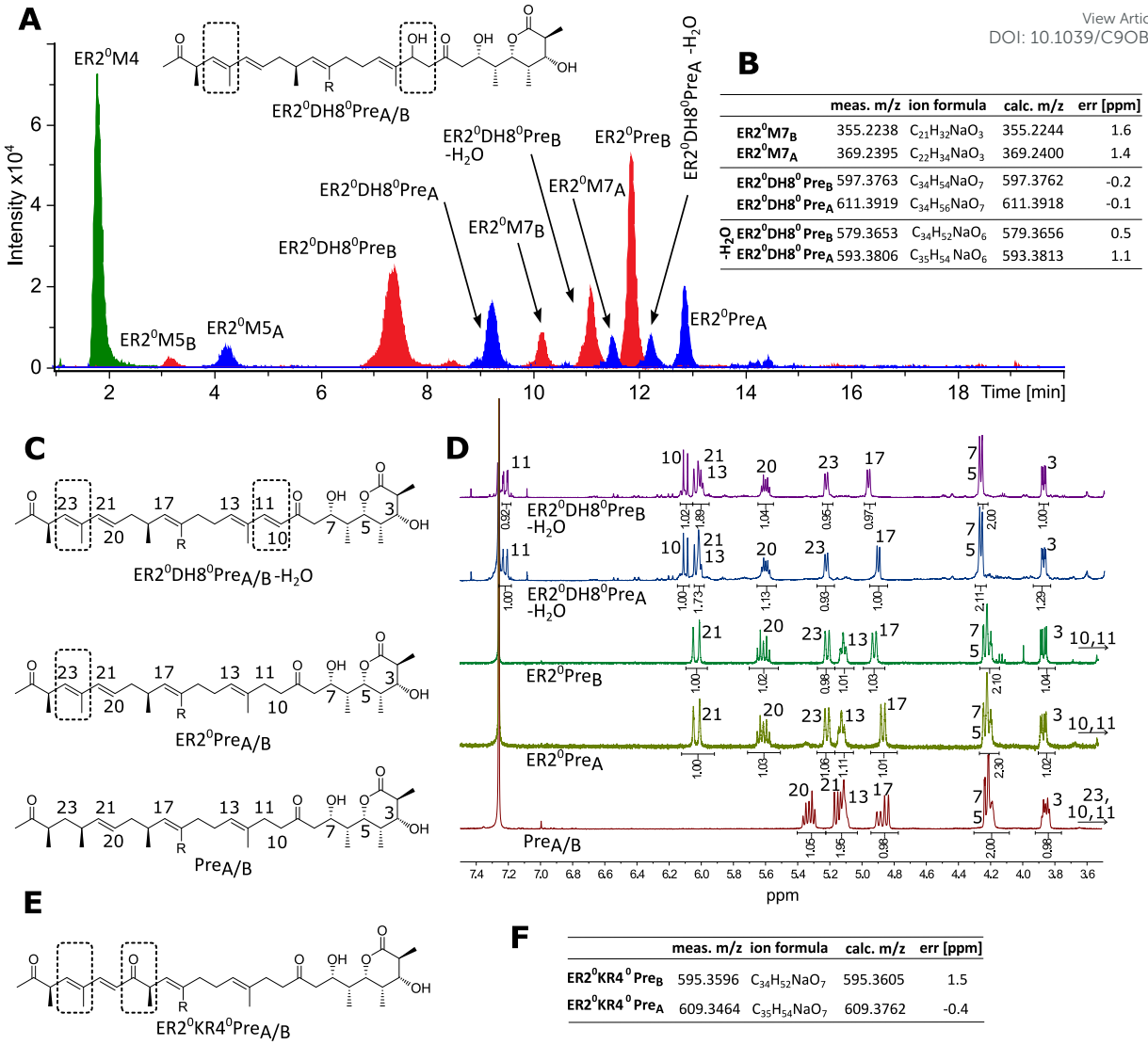

	meas. m/z	ion formula	calc. m/z	err [ppm]
ER2⁰M7B	355.2238	$C_{21}H_{32}NaO_3$	355.2244	1.6
ER2⁰M7A	369.2395	$C_{22}H_{34}NaO_3$	369.2400	1.4
ER2⁰DH8⁰PreB	597.3763	$C_{34}H_{54}NaO_7$	597.3762	-0.2
ER2⁰DH8⁰PreA	611.3919	$C_{34}H_{56}NaO_7$	611.3918	-0.1
-H2O ER2⁰DH8⁰PreB	579.3653	$C_{34}H_{52}NaO_6$	579.3656	0.5
-H2O ER2⁰DH8⁰PreA	593.3806	$C_{35}H_{54}NaO_6$	593.3813	1.1

	meas. m/z	ion formula	calc. m/z	err [ppm]
ER2⁰KR4⁰PreB	595.3596	$C_{34}H_{52}NaO_7$	595.3605	1.5
ER2⁰KR4⁰PreA	609.3464	$C_{35}H_{54}NaO_7$	609.3762	-0.4

Figure 4: A. Extracted ion chromatograms ([M+Na]$^+$ ± 0.005 m/z) showing the hop-off products released from the assembly line in a fermentation of *S. cinnamonensis* A495 ER2^{0}DH8^0. The redox derivatives of premonensin carrying two alterations are labelled as ER2^{0}DH8^{0}Pre$_{A/B}$. Driven by conjugation, spontaneous dehydratization was found via HRMS analysis. **B.** HRMS data of the specific products in ER2^{0}DH8^{0}Pre$_{A/B}$. Intermediates ER2^{0}M7$_{A/B}$ are found in this double-mutant while it was not detected in fermentations of the ER2^0 variant, presumably due to an additional rate-limitation introduced by the second mutation. **C.** Structural comparison of the dehydratized double mutant product ER2^{0}DH8^{0}Pre$_{A/B}$, ER2^{0}Pre$_{A/B}$ and native Pre$_{A/B}$. Numbers indicate ^{1}H-NMR signals as highlighted in **D.** Excerpt of the ^{1}H-NMR spectra of premonensin A/B and its ER2$^0{}_{A/B}$ and dehydratized ER2^{0}DH8$^0{}_{A/B}$ derivatives in the region between 3.5 and 7.5 ppm. The signals are numbered according to the atom numbers in **C**. A full NMR-based characterization is found in SI chapter 6. **E.** Structure of the second derivative produced by a double mutant, however, in very low abundancies **F.** HRMS data on the final products released from the assembly line in a fermentation of *S. cinnamonensis* A495 ER2^{0}KR4^0. Additional MS-characterization is shown in the SI chapter 5.

A 1.8-L fermentation of *S. cinnamonensis* A495 ER2^{0}DH8^0 in SM-16 medium yielded 1.0 mg and 0.7 mg of the B and A forms, respectively, after flash chromatography and preparative HPLC. The product was identified by LC-HRMS and 1D- and 2D-NMR characterization as the dehydratization product of premonensin ER2^{0}DH8^0 (Fig. 4C). The key structural motifs were evident from the NMR signals of the newly introduced vinylic protons and confirmed by 2D-NMR couplings (Fig. 4D). The proton signal at C11 is shifted downfield strongly, reflecting the conjugation that led to the dehydratization of the primary products ER2^{0}DH8^{0}Pre$_{A/B}$. Assignment was carried out via the long-range dd-multiplicity of the signal (see SI chapter 6 for full NMR characterization).

View Article Online
DOI: 10.1039/C9OB00831D

The analysis showed that the combination of mutations in the premonensin assembly is feasible, provided the single mutations give rise to the respective product. In the case of DH5^0, the single mutation delivered the final product in very low abundance and in combination with ER2^0, no fermentation product was detectable. In analogy to the first generation of redox derivatives, hop-off products were found in all doubly-mutated variants, indicating similar rate-limitations; however, the individual population of modules can vary. Furthermore, extensive modification of reduced polyketides can lead to an intrinsic chemical instability of the new-to-nature products, which limits the scope of engineered biosynthesis.

Potential Limitations in Precursor-directed Extender Unit Modification

In addition to mutagenesis-induced redox derivatizations, structural alterations in premonensin and monensin were described to be amendable by precursor-directed biosynthesis.[8-10, 26, 27] Consequently, synthetic extender unit analogues were accepted by monAT5 and incorporated into the polyketide backbone. We investigated the incorporation of synthetic malonic acid-based extender units into premonensin to reveal possible limitations of precursor-directed derivatization.

S. cinnamonensis A495 was fermented in the presence of allyl(All)-, propargyl(Prg)-, propyl(Pr)-, butyl(Bu)-, and chloropropyl(Cl)-substituted malonic acid diethyl ester, as described previously. As expected, all previously reported corresponding premonensin derivatives (Pre_{All}, Pre_{Prg}, Pre_{Pr} and Pre_{Bu}) were detected by LC-HRMS, furthermore, very small quantities of the previously undescribed chloropropylpremonensin (Pre_{Cl}, Figure S15, Table S50, S51).

The experiments on the premonensin redox derivatives suggested a selectivity filter in modules directly or further downstream of a mutated PKS domain. This led us to the expectation that passing the M5-intermediate carrying a non-native side chain downstream or its elongation in module 6 might be a bottleneck, resulting in an accumulation of released intermediate derivatives in the feeding experiments. Contradictory to these expectations, no over-proportional intensities of those hop-off products were detected (for chromatograms see SI chapter 4). Analysis of most feeding experiments, besides the ones leading to Pre_{Cl} and Pre_{Bu}, showed an intermediate pattern comparable to the control fermentation of *S. cinnamonensis* A495 with an apparent slight tendency towards the accumulation of the respective M8-11 intermediates and a concomitantly lower abundancy in modules 5-7. In fermentations resulting in trace amounts of Pre_{Cl}, intermediate $M10_{Cl}$ was the only detectable one and Pre_{Bu} formation was accompanied by the detectable release of the late-stage intermediates $M8_{Bu}$, $M10_{Bu}$ and $M11_{Bu}$ (Fig. 5).

View Article Online
DOI: 10.1039/C9OB00831D

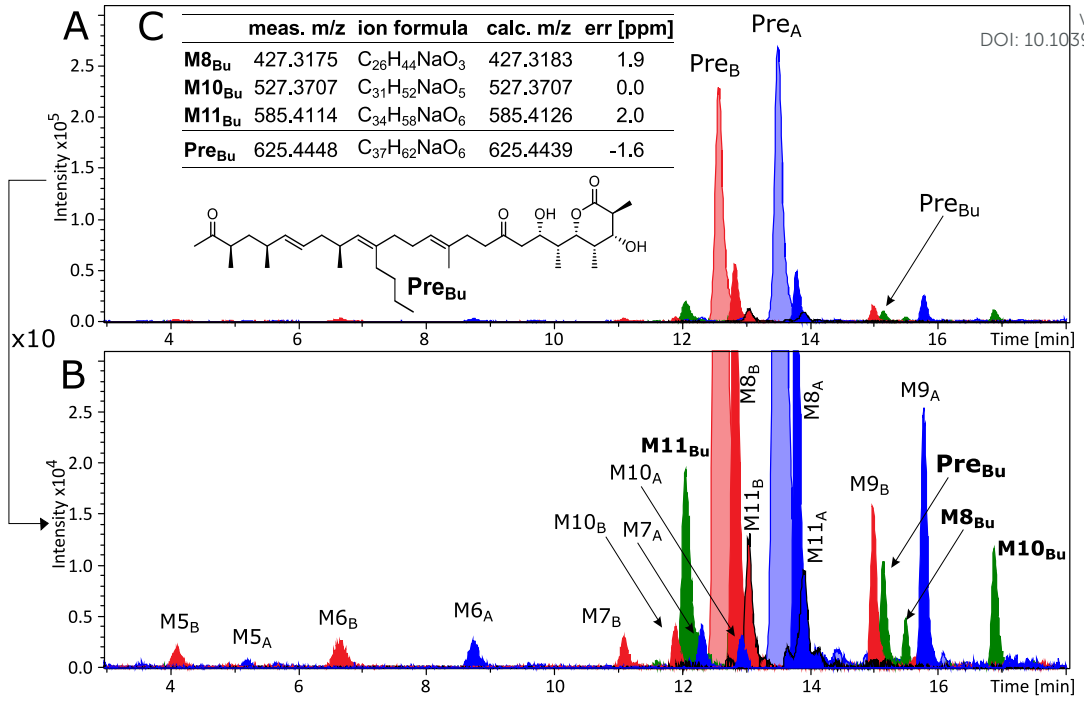

	meas. m/z	ion formula	calc. m/z	err [ppm]
$M8_{Bu}$	427.3175	$C_{26}H_{44}NaO_3$	427.3183	1.9
$M10_{Bu}$	527.3707	$C_{31}H_{52}NaO_5$	527.3707	0.0
$M11_{Bu}$	585.4114	$C_{34}H_{58}NaO_6$	585.4126	2.0
Pre_{Bu}	625.4448	$C_{37}H_{62}NaO_6$	625.4439	-1.6

Figure 5: A. Extracted ion chromatogram ($[M+Na]^+$ ± 0.005) indicating the final products and hop-off intermediates in an extract from a fermentation of *S. cinnamonensis* A495 supplemented with 10 mM of diethyl butylmalonate. Comparably small amounts of butylpremonensin (Pre_{Bu}) were formed via incorporation of the new-to-nature extender unit in module 5. Hop-off products are shown in the corresponding color of the final product (premonensin A: blue; premonensin B: red; butylpremonensin: green). **B.** Ten-times extension of the chromatogram showing hop-off products released from different modules. **C.** HRMS data of Pre_{Bu} and the detectable hop-off products released from modules 8, 10 and 11.

The biosynthetic flow towards premonensin is split into three competing products, depending on which artificial building block is incorporated in module 5 by the promiscuous AT domain. In contrast to mutagenesis-induced redox derivatizations, extender unit variations in the monensin assembly line are not limited by selectivity filters in the adjacent module 6. Instead, the machinery in module 6 appears to rely on the built-in selectivity of the AT5 domain and the correct protein-protein interaction in between the two modules. The incorporation of new-to-nature extender units does not lead to an incomplete reduction of the growing chain in module 5, as no irregular intermediates were released above the detection limit. However, a lower abundance of non-natural intermediates generally correlated with an increase of the final derivatized product abundance, pointing at processivity limitations at various positions in the assembly line. These results suggest that the major limitation in the precursor-directed variation of extender units is the competition with endogenous analogues, which requires further engineering of the respective AT domain to achieve an improved shift in specificity.[10, 26, 28-31]

Specificity Sources in PKS Assembly Lines: Trans-acting Hydrolases as Potential Proofreading Enzymes

The results raised the question: Which factor would induce the apparent engineering limitation of the monensin PKS? Different specificity sources in PKS are being currently discussed in various different systems. The intrinsic specificity of KS domains towards an incoming nascent polyketide chain is well described for trans-AT PKS systems.[32-34] Additionally, trans-acting hydrolases in the same sub-family of

View Article Online
DOI: 10.1039/C9OB00831D

PKS were identified which are capable of removing aberrant intermediates from the ACP in the respective module.[35-40]

As discussed in previous studies, downstream domains in PKS assembly lines appear to possess an intrinsic substrate selectivity not only in trans-AT but also in cis-AT systems.[41-43] However, this selectivity does not seem to be equally strong in cis-AT PKS, as it tolerates a derivatization of the nascent polyketide chain in a variety of different cases with moderate yields and cis-AT KS sequences do not strictly correlate with substrate structures.[42, 44, 45] Zhang et al. recently described fingerprint motifs in KS synthase domains,[43] which we find to apply moderately to olefin-accepting KS domains and showed no correlation with any other type of substrate structure in the monensin and related polyether PKS KS domains (for phylogenetic tree and multiple sequence alignment see SI chapter 7). We particularly could not identify a fingerprint motif for β-ketoacyl-accepting KS domains, which would otherwise have explained the poor processivity in KR^0 variants (Figure S50). Furthermore, ACP domains may contribute to selectivity.[35-40]

The observation that a rate-limitation does not necessarily only lie in the neighboring downstream module suggests that in addition to the possible effects of substrate-specific KS domains, one or more presumably trans-acting proofreading enzymes might exist. In *S. cinnamonensis*, these would recognize aberrant intermediates and remove them from the assembly line.

TE I domains are responsible for the acyl chain release of the nascent polyketides in modular PKS.[46-48] However, many modular PKS gene clusters contain supplementary TE genes (referred to as type II TEs or TE II) in close proximity to the PKS genes.[20, 49, 50] Deletion of these genes was shown to decrease the biosynthesis of tylosin[51] and rifamycin,[52] increase the production of precolibactins,[20] while the yields of pikromycin[53] and surfactin[54] were unaffected. *In vitro* studies on type II TEs showed that some are capable of hydrolyzing aberrant acyl-SNAC[49] and acyl-ACP thioesters,[55] assigning them an editorial role.

A closer inspection of the monensin biosynthetic gene cluster in *S. cinnamonensis* showed three different hydrolases with an incompletely studied function in the biosynthetic pathway (Fig. 6A). It has been stated previously that these might act as type II TEs (MonAIX and MonAX)[21, 49] or as lipase (Orf31).[2] We decided to explore the activity of these putative enzymes (Fig. 6A/B) *in vitro* on substrates, which would resemble polyketide biosynthesis intermediates on the triketide stage (Fig. 1C).

View Article Online
DOI: 10.1039/C9OB00831D

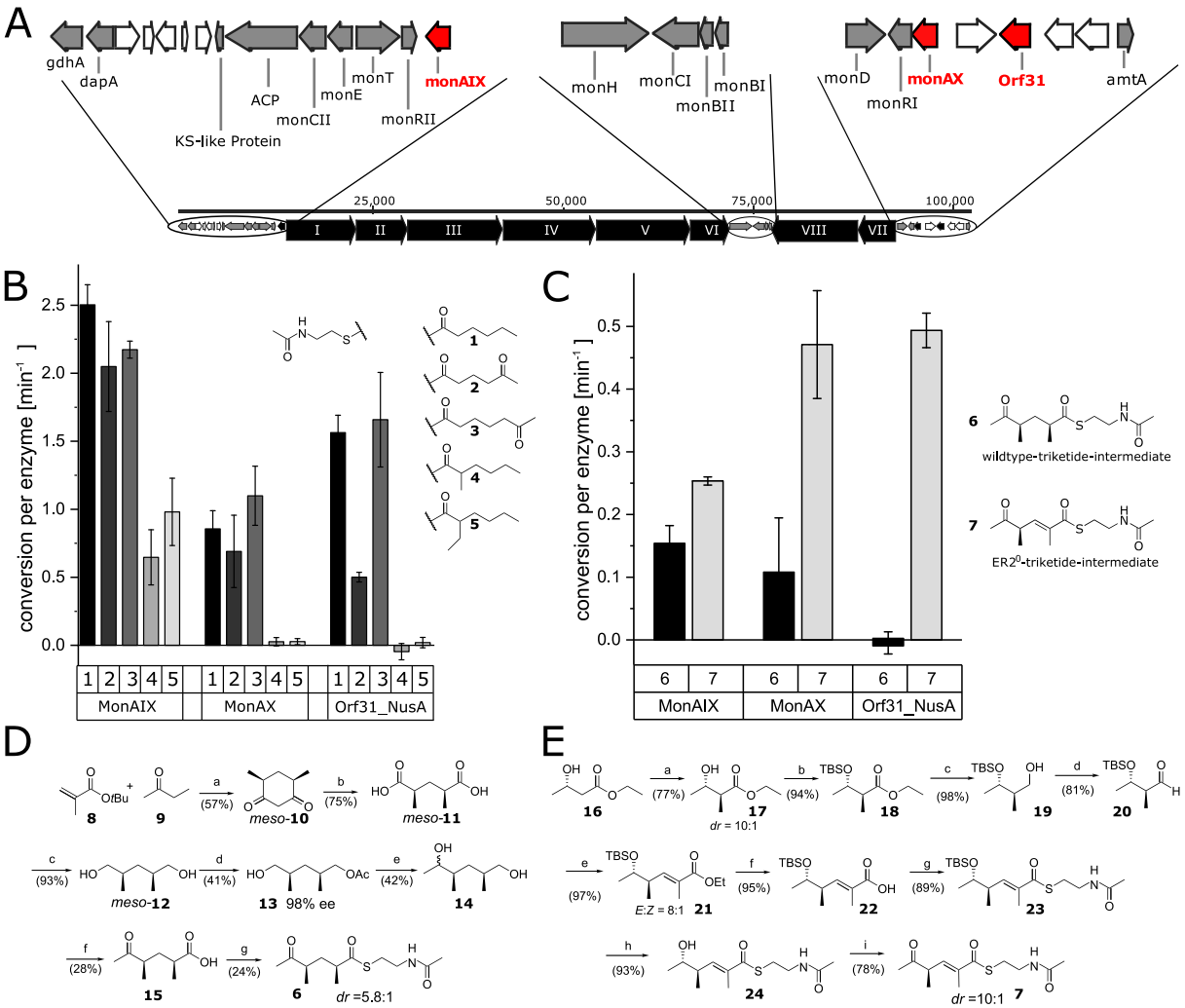

Figure 6: A. Localization of putative hydrolases in the monensin PKS gene cluster.[2] **B**. Activity profiling of the hydrolases using simple model substrates by means of a DTNB assay (SI chapter 8). Error bars result from the standard deviation of three independent measurement; the different substrates are shown in different shades of grey. **C**. Activity of the three hydrolases in the hydrolysis of the SNAC esters of M2 and ER2^{0}M2 to interrogate a possible discrimination of redox variations on the assembly line. **D**. Synthesis of the wild-type triketide intermediate in monensin biosynthesis as a model substrate, corresponding to the M2-intermediate in the biosynthetic assembly line. a) *t*-BuOK, THF, 0 °C to rt, (57%);[56] b) $NaIO_4$, H_2O, 0 °C to rt, (75%);[57] c) $LiAlH_4$, THF, 0 °C to rt, then 65 °C, (93%); d) amano lipase from *Pseudomonas fluorescens*, vinyl acetate, rt (41%, 98% ee, Figure S55, S56);[58] e) 1. DMP, CH_2Cl_2, 0 °C to rt (88%) 2. MeMgBr, Et_2O, 0°C (51%); f) oxalyl chloride, DMSO, Et_3N, CH_2Cl_2, -64 to -30 °C, then $NaClO_2$, Na_2HPO_4, 2-methyl-2-butene, t-BuOH:H_2O (1:1) (28%);[59] g) DPPA, SNAC, Et_3N, DMF, 0°C to rt (24%).[60] *t*BuOK = potassium tert-butoxide, THF = tetrahydrofuran, DMSO = dimethyl sulfoxide, Et_3N = triethylamine, MeMgBr = methyl magnesium bromide, Et_2O = ethoxyethane, DMF = *N*,*N*-dimethylformamide, DPPA = diphenyl phosphoryl azide, SNAC = *N*-acetyl cysteamine, DMP = Dess-Martin periodinane. **E**. Synthesis of the SNAC-activated ER2^0-M2 intermediate as a model substrate. a) LDA, MeI, THF, -65 °C to rt (77%);[61] b) Imidazole, TBS-Cl, DMF, rt (94%);[62] c) DIBAL-H, toluene:CH_2Cl_2 (2:1), -63 to -20 °C (98%); d) oxalyl chloride, DMSO, Et_3N, CH_2Cl_2, -60 °C to rt (81%); e) ethyl 2-(triphenylphosphoranylidene)propionate, toluene, 70 °C (97%);[60] f) K_2CO_3, MeOH:H_2O (3:1), reflux (95%); g) DPPA, SNAC, Et_3N, DMF, 0 °C to rt (89%);[60] h) PPTS, MeOH, 50 °C (93%); i) DMP, CH_2Cl_2, 0 °C (78%). LDA = lithium diisopropylamide, TBS-Cl = tert-butyldimethylsilyl chloride, DIBAL-H = diisobutylaluminium hydride, PPTS: pyridinium p-toluenesulfonate, MeI: iodomethane. Further details on synthetic procedures are found in the SI, chapter 9.

View Article Online
DOI: 10.1039/C9OB00831D

Firstly, the hydrolytic activity of MonAIX, MonAX and Orf31, purified from *E. coli* expression cultures, was monitored on five SNAC-activated thioesters as mimics for the ACP-bound intermediates (Fig. 5B). All three enzymes showed activity on several substrates and hydrolyzed test substrates with different redox patterns and irregular chain length (compounds **1-3**). MonAIX also converted the branched substrates **4** and **5**. In previous reports, MonAIX and MonAX were unsuccessfully tested for activity on longer, fatty acid-like substrates.[21]

The enzymes show a broad activity profile while also revealing some limited substrate specificity. We next decided to interrogate the catalytic properties *in vitro* on more realistic substrates that would resemble intermediates in module 2 of the monensin PKS. Consequently, we chemically synthesized the wild-type intermediate (**6**) and the intermediate **7** from a PKS variant with an inactivated ER2 domain (Fig. 6 D, E), each in the form of the SNAC thioester.

A synthesis of the wild-type thioester was carried out. Stereoselectivity was introduced by a lipase-mediated desymmetrization[58] of the *meso*-intermediate **12**. The analogous ER2^0-triketide was obtained through a 9-step synthesis, starting from ethyl (*S*)-3-hydroxybutyrate **16** (Fig. 6D/E). The stereospecificity required was controlled via a diastereoselective Frater-Seebach alkylation[61] and an *E*-selective Wittig reaction.[60]

Hydrolysis experiments show a difference in the catalytic efficiency of the two compounds between the three enzymes. MonAIX and MonAX accept both substrates, however, slightly prefer the redox derivative ER2^0. Orf31 does not accept the wild-type intermediate as a substrate while hydrolyzing the ER2^0 derivative with significant activity. These *in vitro* results suggest a potential proofreading activity of these enzymes. However, this hypothesis called for *in vivo* verification and, hence, we proceeded with the deletion of all hydrolases in the genome of *S. cinnamonensis* A495.

In Vivo Role of Hydrolases in Premonensin Biosynthesis

Firstly, the three hydrolases were separately in-frame deleted in the chromosome of *S. cinnamonensis* A495. Fermentation of the resulting variants A495 Δ*monAIX* and A495 Δ*orf31* led to insignificant alterations in premonensin productivity in accordance with previous reports of monAIX in the monensin producer.[21] However, while the deletion of *monAX* has been previously reported to lead to a strongly varying drop in monensin productivity, the analogous mutation in the premonensin producer *S. cinnamonensis* A495 Δ*monAX* fully abolished productivity over all four clones tested. In contrast to the properties of the previously reported type II thioesterase clpQ in the colibactin gene cluster,[20] none of the deletions resulted in a decrease in the abundance of intermediates.

We decided to individually delete the hydrolases MonAIX and Orf31 in all variants having a single null mutation of a reductive domain of modules 2 and 6 to identify both module and redox state specificity of a potential proofreading activity. Both modules possess a complete reductive loop with all three types of reductive domains. Furthermore, each of these domains was successfully inactivated in a previous study with strong processivity variations in the resulting PKS.[11]

MonAIX and *orf31* genes were successfully deleted in all variants targeted, except in the case of the *orf31* deletion in the KR6^0 variant. Fermentation of the resulting 11 *S. cinnamonensis* variants revealed no significant alterations in premonensin derivative productivity over at least four independent clones.

View Article Online
DOI: 10.1039/C9OB00831D

The deletion of the two hydrolases were combined in *S. cinnamonensis* A495 Δ*monAIX*Δ*orf31* and its corresponding redox variants in modules 2 and 6. This experiment would reveal a potential complementation of a single deletion by the remaining hydrolase.

Comparative fermentations have not shown an increase in productivity for any premonensin redox derivative after the deletion of one or both of the non-essential hydrolases Orf31 or MonAIX. Furthermore, the relative abundance of intermediates was not affected in any of the clones.

The effect of the deletion of the hydrolases on the incorporation of artificial extender units was investigated in parallel experiments in variants of *S. cinnamonensis* A495 carrying single and combined deletions of *monAIX* and *orf31* using the non-natural malonic acid derivatives listed above. The abundance of the corresponding premonensin derivatives, each normalized to the sum of premonensin A and B, increased in the case of the butyl-substituted extender unit (Figure 7). Alterations were insignificant in the other cases. Pre_{Cl} formation was found in one out of three clones in the control, whereas all three deletion clones gave rise to the derivative.

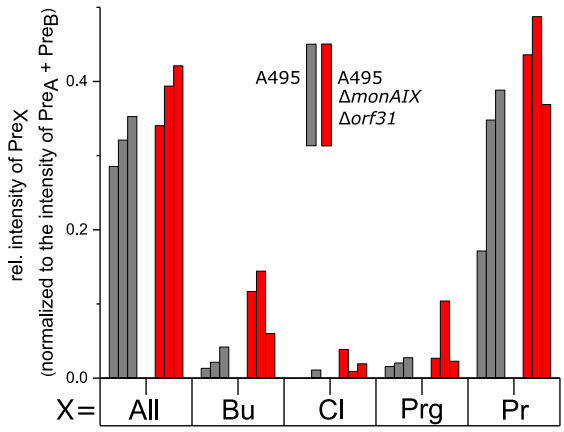

Figure 7: Effect of hydrolase double-deletions on the relative abundance of the side-chain derivatives of premonensin, normalized to the combined abundance of premonensin A and B in the same fermentation extract. The control strain *S. cinnamonensis* A495 and variant *S. cinnamonensis* A495 Δ*monAIX*Δ*orf31* were tested in three independent clones each. Deletion of the hydrolases had a significant positive effect on the productivity level of butyl premonensin ($p = 0.05$). On the other hand, all deletion clones produced the corresponding chloropropyl derivative, while only one wild-type clone delivered measurable quantities of this compound. Both single deletions showed no significant effect.

The relative abundance of derivatized intermediates in each case increased proportionally to the final derivatized product. However, a proofreading activity of a hydrolase would possibly reveal itself in a change in the intermediate pattern upon its deletion. As this is not discernible, the molecular reason for the possibly increased productivity remains elusive and requires further experiments.

CONCLUSION

We here report on the identification of key intermediates in monensin biosynthesis and variously engineered biosynthetic assembly lines.

The experiments highlight a significant substrate specificity in downstream domains as nascent polyketide intermediates with new-to-nature β-keto groups typically accumulate and are not further

View Article Online
DOI: 10.1039/C9OB00831D

processed after the mutated module. Other non-native redox states appear to be converted with lowered processivity instead, leading to a gradual decrease in product formation rather than a complete shut-down of the assembly line.

When the catalytic promiscuity of an AT domain is exploited for the introduction of non-natural extender units, the module directly downstream of this event does not select against this incorporation. Instead, nascent intermediates with aberrant side chains tend to accumulate in distant modules, implying so far nebulous obstacles in substrate channeling.

The detailed mechanism underlying the rate and, thereby, yield limitation in engineered polyketide biosynthesis remains to be identified. The contribution of downstream KS domains and potentially trans-acting hydrolases might turn out to be causative for the decreased yield upon the engineering of polyketide biosynthetic pathways. KS sequence alignments have not yet revealed discernible fingerprint sequences that would identify substrate preferences on a broader basis nor have cis-AT type I PKS gene clusters readily revealed proofreading enzymes.

The results presented in this manuscript suggest that concomitant targeted metabolomics experiments to identify bottlenecks in the artificial system are advisable in each case of engineered polyketide biosynthesis to reveal specific limitations. Counter-strategies will have to be developed, currently on a case-by-case basis, until more enzymological knowledge on PKS is gathered. In contrast to oversimplified earlier views on polyketide assembly lines, cis-AT type I PKS possess a substrate specificity that turns out to limit the engineered biosynthesis of reduced polyketides on a routine basis.

MATERIALS AND METHODS

Chromosomal deletions: Constructs based on pKC1139 were employed for the deletion of the hydrolases.[63] *codA* (*E. coli*) was introduced into pKC1139 and exconjugants cultivated in the presence of 5-fluorocytosin to enable rapid selection for the second crossover.[64] After selection, suitable colonies were identified by colony PCR and sequencing. Oligonucleotide sequences are shown in the SI chapter 8.

Fermentation: Precultures in TSB medium (2 ml, 300 µg/ml phosphomycin, 2 d, 30 °C, 180 rpm) in PP tubes supplied with glass beads were inoculated from colonies on GYM agar. An amount of 15 ml SM16 medium (20 g/L XAD16, 250 ml Erlenmeyer flasks, glass beads, 30 °C, 180 rpm) was inoculated with 5 % preculture and cultivated for 5 d.

Sample preparation: Cell paste and XAD16 resin were collected by centrifugation and frozen at -20 °C. The solids from one flask were extracted with 6 ml ethylacetate (12 h, 19 °C, 150 rpm). The organic layer was subsequently recovered and the solvent removed *in vacuo*. The residue obtained was dissolved in 3 ml acetonitrile (HPLC grade) and stored at -80 °C. Samples were centrifuged (12,000 x g, 4 °C, 30 min) prior to LC-HRMS analysis.

LC-HRMS: An amount of 2 µl or 5 µL (redox derivatives) of each sample was analyzed by LC-HRMS/MS^2. LC-HRMS analysis was run on an Ultimate 3000 HPLC System (consisting of a pump, autosampler, column oven and UV detector) coupled to a compact mass spectrometer (BRUKER DALTONIK GmbH, Life Sciences, Bremen, Germany) using the standard electrospray ionization source. All solvents were LC-MS grade (Chromasolv). A Nucleodur C18 Isis column (Macherey&Nagel, 150/2, 1.8 µm), was used for chromatographic separation. Further details are described in the SI chapter 2.

View Article Online
DOI: 10.1039/C9OB00831D

Author contributions

F. S. and S. K. conceived the idea and designed the experiments. S. K., M. G., N. P. performed experiments with the help of J. E., D. M., and A. I.-A., M. G. and F. S. conducted the data analysis with the help from S. K., and F. S. and M. G. wrote the manuscript with input from all authors. F. S. supervised the research.

Conflicts of interest

There are no conflicts to declare.

Acknowledgments

Christian Merten (RUB) is thanked for VCD-analysis of compound **13.** Part of this research was funded by the DFG Research Training Group GRK 2341 “Microbial Substrate Conversion” (MiCon). M. G. and A. I.-A. are fellows of the International Max Planck Research School of Chemical and Molecular Biology and M. G. thanks the Studienstiftung des deutschen Volkes. N. P. is a fellow of the Manchot Foundation. D. M. and F. S. acknowledge the German Research Foundation for support within the Cluster of Excellence RESOLV EXC1069. This work is supported by the „Center for Solvation Science ZEMOS“ funded by the German Federal Ministry of Education and Research BMBF and by the Ministry of Culture and Research of Nord Rhine-Westphalia.

References

1. J. Staunton and K. J. Weissman, *Natural Product Reports*, 2001, **18**, 380-416.
2. M. Oliynyk, C. B. Stark, A. Bhatt, M. A. Jones, Z. A. Hughes-Thomas, C. Wilkinson, Z. Oliynyk, Y. Demydchuk, J. Staunton and P. F. Leadlay, *Mol Microbiol*, 2003, **49**, 1179-1190.
3. Z. A. Hughes-Thomas, C. B. W. Stark, I. U. Bohm, J. Staunton and P. F. Leadlay, *Angew Chem Int Edit*, 2003, **42**, 4475-4478.
4. C. Hertweck, *Angewandte Chemie International Edition*, 2009, **48**, 4688-4716.
5. B. Lowry, X. Li, T. Robbins, D. E. Cane and C. Khosla, *ACS Central Science*, 2016, **2**, 14-20.
6. K. J. Weissman and P. F. Leadlay, *Nature Reviews Microbiology*, 2005, **3**, 925.
7. A. Bhatt, C. B. W. Stark, B. M. Harvey, A. R. Gallimore, Y. A. Demydchuk, J. B. Spencer, J. Staunton and P. F. Leadlay, *Angewandte Chemie International Edition*, 2005, **44**, 7075-7078.
8. D. Möller, S. Kushnir, M. Grote, A. Ismail-Ali, K. R. M. Koopmans, F. Calo, S. Heinrich, B. Diehl and F. Schulz, *Lett. Appl. Microbiol.*, 2018, **67**, 226-234.
9. A. Ismail-Ali, E. K. Fansa, N. Pryk, S. Yahiaoui, S. Kushnir, M. Pflieger, A. Wittinghofer and F. Schulz, *Org. Biomol. Chem.*, 2016, **14**, 7671-7675.
10. K. Bravo-Rodriguez, A. F. Ismail-Ali, S. Klopries, S. Kushnir, S. Ismail, E. K. Fansa, A. Wittinghofer, F. Schulz and E. Sanchez-Garcia, *Chembiochem*, 2014, **15**, 1991-1997.
11. S. Kushnir, U. Sundermann, S. Yahiaoui, A. Brockmeyer, P. Janning and F. Schulz, *Angewandte Chemie International Edition*, 2012, **51**, 10664-10669.
12. C. Bayly and V. Yadav, *Molecules*, 2017, **22**, 235.
13. E. Kalkreuter and G. J. Williams, *Current Opinion in Microbiology*, 2018, **45**, 140-148.
14. M. Klaus and M. Grininger, *Natural Product Reports*, 2018, DOI: 10.1039/C8NP00030A.
15. K. J. Weissman, *Natural Product Reports*, 2016, **33**, 203-230.
16. M. Tosin, L. Betancor, E. Stephens, W. M. Ariel Li, J. B. Spencer and P. F. Leadlay, *ChemBioChem*, 2010, **11**, 539-546.
17. J. Havemann, M. E. Yurkovich, R. Jenkins, S. Harringer, W. Tao, S. Wen, Y. Sun, P. F. Leadlay and M. Tosin, *Chemical Communications*, 2017, **53**, 1912-1915.
18. M. Tosin, Y. Demydchuk, J. S. Parascandolo, C. Blasco Per, F. J. Leeper and P. F. Leadlay, *Chemical Communications*, 2011, **47**, 3460-3462.
19. J. Moldenhauer, X.-H. Chen, R. Borriss and J. Piel, *Angewandte Chemie International Edition*, 2007, **46**, 8195-8197.
20. Z.-R. Li, J. Li, J.-P. Gu, J. Y. H. Lai, B. M. Duggan, W.-P. Zhang, Z.-L. Li, Y.-X. Li, R.-B. Tong, Y. Xu, D.-H. Lin, B. S. Moore and P.-Y. Qian, *Nature Chemical Biology*, 2016, **12**, 773.
21. B. M. Harvey, H. Hong, M. A. Jones, Z. A. Hughes-Thomas, R. M. Goss, M. L. Heathcote, V. M. Bolanos-Garcia, W. Kroutil, J. Staunton, P. F. Leadlay and J. B. Spencer, *ChemBioChem*, 2006, **7**, 1435-1442.
22. S. Ojanperä, A. Pelander, M. Pelzing, I. Krebs, E. Vuori and I. Ojanperä, *Rapid Communications in Mass Spectrometry*, 2006, **20**, 1161-1167.
23. A. L. Rockwood, S. L. Van Orden and R. D. Smith, *Analytical Chemistry*, 1995, **67**, 2699-2704.
24. A. Tenhosaari, *Organic Mass Spectrometry*, 1988, **23**, 236-239.
25. J. Wu, T. J. Zaleski, C. Valenzano, C. Khosla and D. E. Cane, *Journal of the American Chemical Society*, 2005, **127**, 17393-17404.
26. K. Bravo-Rodriguez, S. Klopries, Kyra R. M. Koopmans, U. Sundermann, S. Yahiaoui, J. Arens, S. Kushnir, F. Schulz and E. Sanchez-Garcia, *Chemistry & Biology*, 2015, **22**, 1425-1430.
27. M. Grote and F. Schulz, *ChemBioChem*, 2019, **in press**.
28. I. Koryakina, C. Kasey, J. B. McArthur, A. N. Lowell, J. A. Chemler, S. Li, D. A. Hansen, D. H. Sherman and G. J. Williams, *ACS Chemical Biology*, 2017, **12**, 114-123.
29. E. M. Musiol-Kroll, F. Zubeil, T. Schafhauser, T. Härtner, A. Kulik, J. McArthur, I. Koryakina, W. Wohlleben, S. Grond, G. J. Williams, S. Y. Lee and T. Weber, *ACS Synthetic Biology*, 2017, **6**, 421-427.
30. C. C. Ladner and G. J. Williams, *Journal of Industrial Microbiology & Biotechnology*, 2016, **43**, 371-387.

View Article Online
DOI: 10.1039/C9OB00831D

31. U. Sundermann, K. Bravo-Rodriguez, S. Klopries, S. Kushnir, H. Gomez, E. Sanchez-Garcia and F. Schulz, *ACS Chemical Biology*, 2013, **8**, 443-450.
32. M. Jenner, S. Frank, A. Kampa, C. Kohlhaas, P. Pöplau, G. S. Briggs, J. Piel and N. J. Oldham, *Angewandte Chemie International Edition*, 2013, **52**, 1143-1147.
33. J. Piel, *Natural Product Reports*, 2010, **27**, 996-1047.
34. M. Jenner, J. P. Afonso, H. R. Bailey, S. Frank, A. Kampa, J. Piel and N. J. Oldham, *Angewandte Chemie*, 2015, **127**, 1837-1841.
35. K. J. Weissman, *Natural Product Reports*, 2015, **32**, 436-453.
36. C. Anselmi, M. Grininger, P. Gipson and J. D. Faraldo-Gómez, *Journal of the American Chemical Society*, 2010, **132**, 12357-12364.
37. S. Dutta, J. R. Whicher, D. A. Hansen, W. A. Hale, J. A. Chemler, G. R. Congdon, A. R. H. Narayan, K. Hakansson, D. H. Sherman, J. L. Smith and G. Skiniotis, *Nature*, 2014, **510**, 512-517.
38. J. R. Whicher, S. Dutta, D. A. Hansen, W. A. Hale, J. A. Chemler, A. M. Dosey, A. R. H. Narayan, K. Hakansson, D. H. Sherman, J. L. Smith and G. Skiniotis, *Nature*, 2014, **510**, 560-564.
39. K. J. Weissman, *Nat Chem Biol*, 2014, **11**, 660-670.
40. C. Nguyen, R. W. Haushalter, D. J. Lee, P. R. L. Markwick, J. Bruegger, G. Caldara-Festin, K. Finzel, D. R. Jackson, F. Ishikawa, B. O/'Dowd, J. A. McCammon, S. J. Opella, S.-C. Tsai and M. D. Burkart, *Nature*, 2014, **505**, 427-431.
41. T. Nguyen, K. Ishida, H. Jenke-Kodama, E. Dittmann, C. Gurgui, T. Hochmuth, S. Taudien, M. Platzer, C. Hertweck and J. Piel, *Nature Biotechnology*, 2008, **26**, 225.
42. A. C. Murphy, H. Hong, S. Vance, R. W. Broadhurst and P. F. Leadlay, *Chemical Communications*, 2016, **52**, 8373-8376.
43. L. Zhang, T. Hashimoto, B. Qin, J. Hashimoto, I. Kozone, T. Kawahara, M. Okada, T. Awakawa, T. Ito, Y. Asakawa, M. Ueki, S. Takahashi, H. Osada, T. Wakimoto, H. Ikeda, K. Shin-ya and I. Abe, *Angewandte Chemie International Edition*, 2017, **56**, 1740-1745.
44. H. Jenke-Kodama, T. Börner and E. Dittmann, *PLOS Computational Biology*, 2006, **2**, e132.
45. A. Ginolhac, C. Jarrin, P. Robe, G. Perrière, T. M. Vogel, P. Simonet and R. Nalin, *Journal of Molecular Evolution*, 2005, **60**, 716-725.
46. R. Aggarwal, P. Caffrey, P. F. Leadlay, C. J. Smith and J. Staunton, *J Chem Soc Chem Comm*, 1995, DOI: DOI 10.1039/c39950001519, 1519-1520.
47. K. J. Weissman, C. J. Smith, U. Hanefeld, R. Aggarwal, M. Bycroft, J. Staunton and P. F. Leadlay, *Angewandte Chemie International Edition*, 1998, **37**, 1437-1440.
48. R. Pieper, G. Luo, D. E. Cane and C. Khosla, *Nature*, 1995, **378**, 263-266.
49. M. L. Heathcote, J. Staunton and P. F. Leadlay, *Chemistry & Biology*, 2001, **8**, 207-220.
50. L. Du and L. Lou, *Natural Product Reports*, 2010, **27**, 255-278.
51. A. R. Butler, N. Bate and E. Cundliffe, *Chemistry & Biology*, 1999, **6**, 287-292.
52. Y. Doi-Katayama, Y. J. Yoon, C. Y. Choi, T. W. Yu, H. G. Floss and C. R. Hutchinson, *Journal of Antibiotics*, 2000, **53**, 484-495.
53. S. Chen, J. B. Roberts, Y. Xue, D. H. Sherman and K. A. Reynolds, *Gene*, 2001, **263**, 255-264.
54. P. Cosmina, F. Rodriguez, F. Ferra, G. Grandi, M. Perego, G. Venema and D. Sinderen, *Molecular microbiology*, 1993, **8**, 821-831.
55. B. S. Kim, T. A. Cropp, B. J. Beck, D. H. Sherman and K. A. Reynolds, *Journal of Biological Chemistry*, 2002, **277**, 48028-48034.
56. T. Ishikawa, R. Kadoya, M. Arai, H. Takahashi, Y. Kaisi, T. Mizuta, K. Yoshikai and S. Saito, *The Journal of Organic Chemistry*, 2001, **66**, 8000-8009.
57. M. L. Wolfrom and J. M. Bobbitt, *Journal of the American Chemical Society*, 1956, **78**, 2489-2493.
58. J. S. Yadav, D. N. Chary, N. N. Yadav, S. Sengupta and B. V. S. Reddy, *Helv Chim Acta*, 2013, **96**, 1968-1977.
59. X. Guo, T. G. Liu, C. R. Valenzano, Z. X. Deng and D. E. Cane, *Journal of the American Chemical Society*, 2010, **132**, 14694-14696.

View Article Online
DOI: 10.1039/C9OB00831D

60. K. Kinoshita, P. G. Williard, C. Khosla and D. E. Cane, *Journal of the American Chemical Society*, 2001, **123**, 2495-2502.
61. D. Gallenkamp and A. Fürstner, *Journal of the American Chemical Society*, 2011, **133**, 9232-9235.
62. J. C. Barrish, H. L. Lee, T. Mitt, G. Pizzolato, E. G. Baggiolini and M. R. Uskokovic, *The Journal of Organic Chemistry*, 1988, **53**, 4282-4295.
63. M. Bierman, R. Logan, K. O'Brien, E. T. Seno, R. Nagaraja Rao and B. E. Schoner, *Gene*, 1992, **116**, 43-49.
64. M.-P. Dubeau, M. G. Ghinet, P.-É. Jacques, N. Clermont, C. Beaulieu and R. Brzezinski, *Applied and Environmental Microbiology*, 2009, **75**, 1211-1214.